Available online at BCREC Website: https://bcrec.undip.ac.id

Bulletin of Chemical Reaction Engineering & Catalysis, 13 (1), 2018, 57-73

Research Article

Syngas Production from Catalytic CO_2 Reforming of CH_4 over $CaFe_2O_4$ Supported Ni and Co Catalysts: Full Factorial Design Screening

M. Anwar Hossain[1], Bamidele V. Ayodele[1], Chin Kui Cheng[1,2,3], Maksudur R. Khan[1,2*]

[1]Faculty of Chemical & Natural Resources Engineering, Universiti Malaysia Pahang, Lebuhraya Tun Razak, 26300 Gambang Kuantan, Pahang, Malaysia
[2]Rare Earth Research Centre, Universiti Malaysia Pahang, Lebuhraya Tun Razak, 26300 Gambang Kuantan, Pahang, Malaysia
[3]Center of Excellence for Advanced Research in Fluid Flow, Universiti Malaysia Pahang, Lebuhraya Tun Razak, 26300 Gambang Kuantan, Pahang, Malaysia

Received: 5th May 2017; Revised: 8th August 2017; Accepted: 9th August 2017
Available online: 22nd January 2018; Published regularly: 2nd April 2018

Abstract

In this study, the potential of dry reforming reaction over $CaFe_2O_4$ supported Ni and Co catalysts were investigated. The $Co/CaFe_2O_4$ and $Ni/CaFe_2O_4$ catalysts were synthesized using wet impregnation method by varying the metal loading from 5-15 %. The synthesized catalysts were tested in methane dry reforming reaction at atmospheric pressure and reaction temperature ranged 700-800 ^oC. The catalytic performance of the catalysts based on the initial screening is ranked as $5\%Co/CaFe_2O_4 < 10\%Co/CaFe_2O_4 < 5\%Ni/CaFe_2O_4 < 10\%Ni/CaFe_2O_4$ according to their performance. The $Ni/CaFe_2O_4$ catalyst was selected for further investigation using full factorial design of experiment. The interaction effects of three factors namely metal loading (5-15 %), feed ratio (0.4-1.0), and reaction temperature (700-800 ^oC) were evaluated on the catalytic activity in terms of CH_4 and CO_2 conversion as well as H_2 and CO yield. The interaction between the factors showed significant effects on the catalyst performance at metal loading, feed ratio and reaction temperature of 15 %, 1.0, and 800 ^oC. respectively. The 15 wt% $Ni/CaFe_2O_4$ was subsequently characterized by Thermogravimetric (TGA), X-ray Diffraction (XRD), Field Emission Scanning Electron Microscopy (FESEM), Energy Dispersive X-ray Spectroscopy (EDX), X-ray Photoelectron Spectroscopy (XPS), N_2-physisorption, Temperature Programmed Desorption (TPD)-NH_3, TPD-CO_2, and Fourier Transform Infra Red (FTIR) to ascertain its physiochemical properties. This study demonstrated that the $CaFe_2O_4$ supported Ni catalyst has a good potential to be used for syngas production via methane dry reforming.

Keywords: Cobalt; Nickel; $CaFe_2O_4$; Methane dry reforming; Syngas

How to Cite: Hossain, M.A., Ayodele, B.V., Cheng, C.K., Khan, M.R. (2018). Syngas Production from Catalytic CO_2 Reforming of CH_4 over $CaFe_2O_4$ Supported Ni and Co Catalysts: Full Factorial Design Screening. *Bulletin of Chemical Reaction Engineering & Catalysis*, 13 (1): 57-73 (doi:10.9767/bcrec.13.1.1197.57-73)

Permalink/DOI: https://doi.org/10.9767/bcrec.13.1.1197.57-73

1. Introduction

The mitigation of greenhouse gases such as CH_4 and CO_2 which contribute about 72 % and 7 %, respectively, to "greenhouse effect" has attracted growing interest in the last one decade [1]. Several methods such as carbon capture and storage, energy efficiency and conservation, negative CO_2 emission and catalytic reforming of methane have been explored to mitigate greenhouse effect [2-4]. Among these options,

* Corresponding Author.
E-mail: mrkhancep@yahoo.com (Khan, M.R.)
Telp.: +609 5492872, Fax.: +609 5492889

methane dry reforming is a promising option for the mitigation of greenhouse effects as it utilizes CH_4 and CO_2, the two prominent components of greenhouse gases [5]. Besides, methane dry reforming is a potential route for the production of synthesis gas (syngas) as represented in Equation (1) [6].

$$CH_4 + CO_2 \rightarrow 2CO + 2H_2 \quad \Delta H=247 \text{ kJ.mol}^{-1} \quad (1)$$

The production of syngas with unity molar ratio is theoretical favored by methane dry reforming, hence the suitability of the syngas as chemical intermediates for the production of oxygenated fuels [7]. However, one of the major constraints with the methane dry reforming is catalyst deactivation via sintering and cooking due to the highly endothermic nature of the reaction [8,9].

Researchers have shown much effort in developing carbon resistant catalysts mostly from noble and transition metals such as Pt, Rh, Ru, Co, and Ni. Extensive review by [10] shows that noble metals are typically much more carbon resistant compared to Co and Ni-based catalyst in methane dry reforming but are expensive and might not be economical for scale up. On the contrary, Co and Ni-based catalysts are inexpensive and show comparable activity with the noble metals [11,12]. The catalytic performance of Co- and Ni-based can be enhanced using suitable supports. Supports such as Al_2O_3, CeO_2, SiO_2, and MgO have been widely explored for the synthesis of Co and Ni-catalysts [13-16]. These catalysts showed various degrees of catalytic performance. However, extensive literature search has shown that $CaFe_2O_4$ which has good acidicity and basicity properties has only been used as catalysts in processes such as photo-degradation of methylene blue as well as in biodiesel production [17,18]. To the best of the authors' knowledge, there is presently no literature on the use of $CaFe_2O_4$ as support for synthesis of Co- and Ni-based catalyst for methane dry reforming. Therefore, the aim of this study was to investigate the initial screening of Co and Ni supported on $CaFe_2O_4$ for methane dry reforming. The best performing catalyst in terms of the reactants conversion and products yields was subsequently characterized using different instruments techniques, such as: TGA, XRD, EDX, XPS, N_2 physisorption, and FTIR, to establish its physiochemical properties. To further explore its potential as dry reforming catalyst, a further screening of the catalyst was performed using full factorial design by considering factors such as metal loadings, feed (CH_4: CO_2) ratio and reaction temperature.

2. Materials and Methods

2.1 Synthesis of catalysts

Prior to the synthesis of the Co- and Ni/$CaFe_2O_4$ catalysts, the $CaFe_2O_4$ support was prepared by sol-gel technique reported elsewhere [17]. In a typical synthesis, a stoichiometric ratio of $Ca(NO_3)_2.4H_2O$ and $Fe(NO_3)_3.9H_2O$ were mixed in 30 % aqueous NH_3 solution, and the mixture was stirred at room temperature for 24 h. The solution was then slowly heated to 80 ^oC and maintained at that temperature level until the water evaporated. The resulting brown dry gel-like slurry was calcined at 450 ^oC for 2 h followed by heat treatment at 900 ^oC for 10 h using muffle furnace to obtained $CaFe_2O_4$ powder. Finally, $CaFe_2O_4$ powders were crushed in the mortar to obtain fine particle size. Thereafter, Ni/CaF_2O_4 was synthesized with metal loading of 5-15 wt% using wet-impregnation method. Required amount of $Ni(NO_3)_2.6H_2O$ precursor was dissolved in aqueous solution and 1 g of $CaFe_2O_4$ was added to the solution under stirring for 3 h. Subsequently, the slurry was oven dried for 24 h at 120 ^oC, crushed and finally calcined at 800 ^oC for 5 h. Similarly, Co/$CaFe_2O_4$ with metal loading of 5-10 wt% was synthesized using the same method mentioned above. The $Co(NO_3)_2.6H_2O$ was used as precursor for this purpose. All the reagents were analytical grade (99.99 % purity, Sigma-Aldrich, USA) and were used as received without further purification.

2.2 Pre-screening of the Co/$CaFe_2O_4$ and Ni/$CaFe_2O_4$ catalysts

Prior to the full factorial design of experiment, a preliminary experiment was carried out to determine a promising active element from Co and Ni that can be synthesized on the $CaFe_2O_4$ support. The Ni/$CaFe_2O_4$ catalyst was selected for further screening based on its activity in terms of conversion and yield. A full factorial design of the Ni/$CaFe_2O_4$ was performed using Statistica 13 software (Dell incorp.) for the design of experiment. The effect of factors such as metal loading (5-15 %), feed ratio (0.4-1) and reaction temperature (700-800 ^oC) on the CH_4 and CO_2 conversion as well as the H_2 and CO yield. The full factorial design of the Ni/ $CaFe_2O_4$ is depicted in Table 1.

2.3 Catalyst characterization

The catalyst (15%wt Ni/$CaFe_2O_4$) with the best performance was further characterized for its physicochemical properties using different instrument techniques. The thermal analysis showing the changes in the physical and chemical properties of the 15%wt Ni/$CaFe_2O_4$ catalyst as a function of increasing temperature was done using Hitachi simultaneous thermal analyser (STA, 7000 series). The STA has the capacity to simultaneously perform Thermogravimetric Analysis (TGA) and Differential Thermal Analysis (DTA). The uncalcined catalyst sample weighing approximately 6 mg was placed in an alumina pan enclosed in a furnace. The temperature of the furnace was increased from 25 to 900 ^oC at heating rate of 10 ^oC/min in a flow of 50 mL/min of pure N_2. The weight loss (TG) and the differential weight loss (DTG) of the catalyst sample as a function of temperature were estimated. The texture properties of the calcined 15%wt Ni/$CaFe_2O_4$ catalyst in terms of BET specific surface area and BJH pore size distribution were measured by N_2 physisorption method using Accelerated Surface Area and Porosimetric system (ASAP 2020 plus). The catalyst sample was degassed at 253 ^oC for 2 h before the commencement of the N_2 physisorption analysis. The 15wt% Ni/$CaFe_2O_4$ catalyst was characterized for phase identification by X-ray powder diffraction analysis using RIGAKU miniflex II X-ray diffractometer. The Rigaku miniflex XRD (Cu-Kα source with wavelength (λ) of 0.154 nm) is capable of measuring powdered diffraction pattern at 2θ scanning ranged 3 to 145^o. The phase identification of the catalyst from the XRD performed using the latest version of PDXL, RIGAKU full function powder-diffraction analysis software. The topographical and the elemental information of the 15%wt Ni/$CaFe_2O_4$ catalyst were measured using JEOL Field Emission Scanning Electron

Table 1. Full factorial design of the Ni/$CaFe_2O_4$ catalyst

Run No.	Feed ratio	Reaction Temperature (^oC)	Metal loading (%)	CH_4 Conversion (%)	CO_2 Conversion (%)	H_2 yield (%)	CO yield (%)
8	0.4	800	10	38.75	35.68	21.11	23.32
18	0.7	800	15	90.04	87.60	73.42	74.43
6	0.4	750	15	25.82	22.22	16.35	17.70
19	1.0	700	5	23.78	20.35	13.56	16.59
21	1.0	700	15	25.38	21.34	12.45	14.35
23	1.0	750	10	52.76	51.85	27.31	30.77
1	0.4	700	5	25.01	21.96	13.26	14.31
9	0.4	800	15	33.45	30.02	17.22	19.15
26	1.0	800	10	26.11	27.77	14.54	15.06
4	0.4	750	5	35.10	31.62	20.64	22.41
15	0.7	750	15	23.43	20.68	13.54	14.37
17	0.7	800	10	22.99	19.60	13.24	14.56
2	0.4	700	10	39.60	38.98	18.78	19.11
11	0.7	700	10	17.69	14.15	11.12	13.39
3	0.4	700	15	34.48	33.52	20.32	19.44
13	0.7	750	5	59.08	56.97	26.22	28.32
22	1.0	750	5	27.46	23.15	14.14	15.32
24	1.0	750	15	52.76	51.85	27.31	30.77
12	0.7	700	15	19.78	16.31	12.32	13.37
16	0.7	800	5	67.93	66.39	35.35	38.31
20	1.0	700	10	23.78	20.35	13.56	16.59
10	0.7	700	5	62.93	62.34	32.36	33.31
14	0.7	750	10	22.99	19.60	13.24	14.56
27	1.0	800	15	88.63	85.41	70.31	73.21
7	0.4	800	5	30.34	26.32	16.17	15.31
5	0.4	750	10	50.70	47.60	26.43	27.31
25	1.0	800	5	26.11	27.77	14.54	15.06

Microscopy (FESEM) and Energy Dispersive X-ray Spectroscopy (EDX). Perkin Elmer Spectrum BX(II) X-ray Photoelectron Spectrophotometer (XPS) was employed to analyse the bond formations of the 15wt% $Ni/CaFe_2O_4$ catalyst. The XPS analysis was performed using Thermo Fisher K-alpha equipped with monochromatic Al Kα X-ray source. The XPS spectra were collected using aluminium anode (Al-Kα =1486.6 eV) operating at 150 W. The recording of the spectra was done at background pressure of 2×10^{-9} mbar under an ultra-high vacuum (UHV) chamber. The TPD analysis using NH_3 and CO_2 as probing gases were carried out using approximately 60 mg each of the fresh catalyst. Prior to the testing the catalyst was pre-treated in a flow of 20 mL min^{-1} N_2 for 1 h at a heating rate of 10 ^oC min^{-1} up to 50 ^oC at holding time of 30 min. The pre-treated catalyst sample was thereafter purged with He and then cooled down to room temperature. The TPD-NH_3 analysis was done by replacing the He gas with NH_3 and allowed to saturate the samples for 1 h. This was followed by purging the sample with He to remove either excess NH_3 in gas phase or the physisorbed NH_3 on the catalysts. The desorption step was carried out under 20 mL min^{-1} He flows at a heating rate of 20 ^oC min^{-1} from room temperature to 900 ^oC and holding time of 20 min before cooling. The amount of NH_3 desorbed was estimated from the TPD pattern recorded online. The above procedure was repeated for TPD-CO_2 analysis using CO_2 gas in place of the NH_3 gas.

2.4 Catalytic activity test

The schematic diagram of the experimental set-up for the catalytic activity test is represented in Figure 1. The set-up comprised CO_2, CH_4, N_2 and H_2 gases (99.99 % purity). The main reactants for the methane dry reforming are CO_2 and CH_4, while N_2 and H_2 serve as carrier gas and for reduction, respectively. The stainless steel fixed bed continuous reactor was packed with 200 mg of catalysts supported with quartz wool and heated inside a split-tube furnace that was equipped with K-type thermocouple for measurement of the catalytic bed temperature. The catalyst was reduced in 60 mL/min of 20 % H_2 and 80 % N_2 prior to the commencement of the catalytic activity test at 900 ^oC for 1 h. The flow rate of the inlet gas was maintained at 100 mL/min and individually regulated with the aid of Alicat digital mass flow controller (MFC) (Alicat Scientific Inc., USA). The outlet gas composition (CO_2, CH_4, CO and H_2) was measured with gas chromatography (GC) instrument (Agilent Technologies, USA) equipped with thermal conductivity detector (TCD). Two packed columns were used viz. Supelco Molecular Sieve 13x (10 ft. 1/8 in. OD 2 mm ID, 60/80 mesh, Stainless Steel) and Agilent Hayesep DB (30 ft. 1/8 in. OD 2 mm ID, 100/120 mesh, Stainless Steel). Helium (He) gas was used as a carrier with flowrate of 20 mL/min with operating column temperature of 120 ^oC and detector temperature of 150 ^oC (column pressure < 90 psi). Separation and quantification of gas analytes viz.

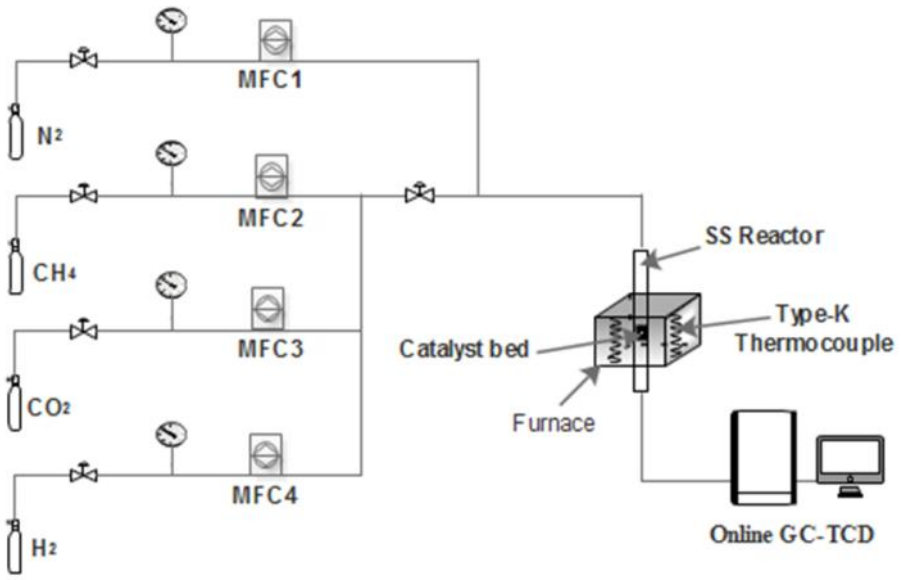

Figure 1. Schematic diagram of experimental set-up for the methane dry reforming over the developed catalysts

H_2, CH_4 and CO_2 were performed using Hayesep DB column; whilst CO were analysed using the Molecular Sieve 13× columns. The conversion of CH_4 and CO_2 as well as the yields of H_2 and CO were calculated using Equations (2)-(5).

$$CH_4 conversion(\%) = \frac{F_{CH_{4in}} - F_{CH_{4out}}}{F_{CH_{4in}}} x100 \quad (2)$$

$$CO_2 conversion(\%) = \frac{F_{CO_{2in}} - F_{CO_{2out}}}{F_{CO_{2in}}} x100 \quad (3)$$

$$H_2 yield = \frac{F_{H_{2out}}}{2F_{CH_{4in}}} x100 \quad (4)$$

$$CO_2 yield = \frac{F_{CO_{out}}}{F_{CH_{4in}} + F_{CO_{2in}}} x100 \quad (5)$$

where F_{CO2in}, F_{CH4in}, F_{CO2out}, and F_{CH4out} are the inlet and outlet molar flow rates of CO_2 and CH_4, respectively. F_{H2} and F_{CO} are the outlet molar flow rates of H_2 and CO, respectively.

3. Results and Discussion

3.1 Pre-screening of the Co- and Ni/$CaFe_2O_4$ catalysts

The pre-screening of the catalyst for dry reforming of methane was performed over the two selected active metals, Co- and Ni-supported on $CaFe_2O_4$ in order to determine which of the active metals can further be selected for subsequent full factorial design. In addition, the catalyst activity of the $CaFe_2O_4$ support was also tested. The pre-screening experiments were carried out considering factors, such as metal loadings (5-10 %), feed ratio (CH_4/CO_2) (0.4-1) and reaction temperature (700-800 °C). The performance of the catalysts was measured based on the conversions of the CH_4 and CO_2 as well as the yields of H_2 and CO. The feed flowrate was fixed at GHSV of 30000 h^{-1}. The activities of the $CaFe_2O_4$ support and the catalysts are shown in Figure 2(a)-(d). It can be seen that $CaFe_2O_4$ shows some activities in term of reaction conversions and the products yields (Figure 2 (a)). The

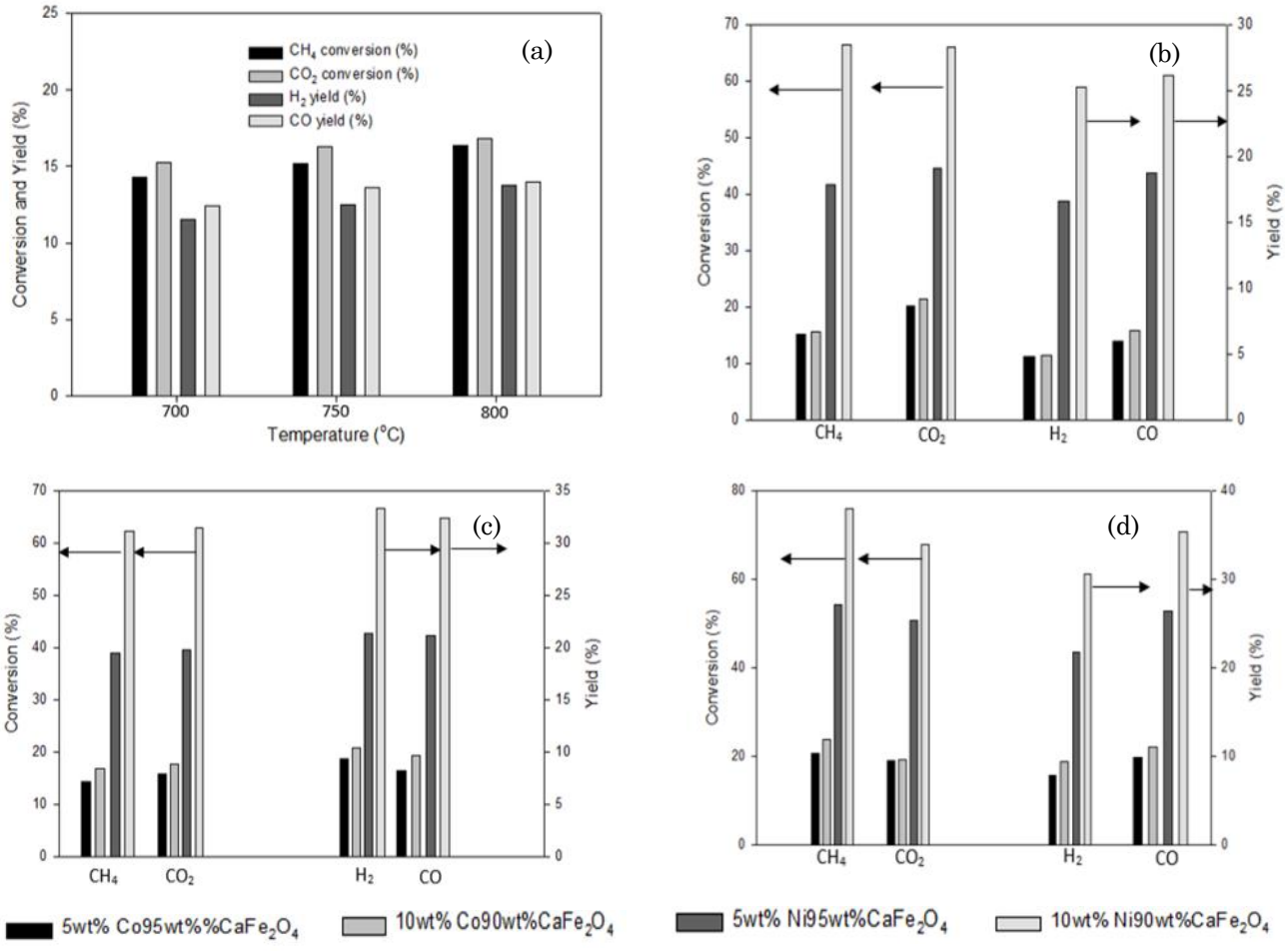

Figure 2. (a) The conversion and yield of $CaFe_2O_4$ and the conversions and yields of screened catalysts at (b) 700 °C, (c) 750 °C, (d) 800 °C

highest values of 16.4 % and 6.8 % were obtained for CH_4 and CO_2 conversions while 13.7 % and 14.10 % were obtained for the H_2 and CO yield respectively at feed (CH_4:CO_2) ratio of and temperature of 800 °C. This implies that the $CaFe_2O_4$ plays significant role in the catalytic activities of the Co and Ni catalysts. The catalysts show an increasing trend with reaction temperature in terms of CH_4 and CO_2 conversions.

Figure 2 (b)-(d) revealed that, CH_4 and CO_2 conversions did not vary much with the metal loading using the Co/$CaFe_2O_4$. This is evident in the overlapping trend obtained for the CH_4 and CO_2 conversions using 5% Co/$CaFe_2O_4$ and 10% Co/$CaFe_2O_4$ catalysts. On the contrary, CH_4 and CO_2 conversions increased with metal loadings and temperature using the Ni/$CaFe_2O_4$. Similar, trends can also be observed in terms of H_2 and CO yields. Hence, the catalytic performance for the pre-screening experiment can be ranked as 5% Co/$CaFe_2O_4$ < 10% Co/$CaFe_2O_4$ < 5% Ni/$CaFe_2O_4$ < 10% Ni/$CaFe_2O_4$ based on their activities in terms of yield and conversion. Based on the performance of the two-screened catalyst, Ni/$CaFe_2O_4$ catalyst was selected for full factorial design of experiment.

3.2 Catalytic performance of Ni/$CaFe_2O_4$ catalyst

The catalytic performance of the 5% Ni/$CaFe_2O_4$, 10% Ni/$CaFe_2O_4$ and 15% Ni/$CaFe_2O_4$ catalysts are depicted in Figures 3-5. Generally, the CH_4 and CO_2 conversion as well as the H_2 and CO yield showed increasing trend with feed ratio and reaction temperature. The catalytic performance of 5% Ni/$CaFe_2O_4$ is depicted in Figure 3. It can be seen that there was slight increase in the CH_4 conversion from 700-800 °C at feed ratio of 0.4 and 0.7 (cf. Figure 3 (a)). However, the CH_4 conversion drastically increased with temperature at unity feed ratio. On the contrary, CO_2 conversion significantly increased with the reaction temperature

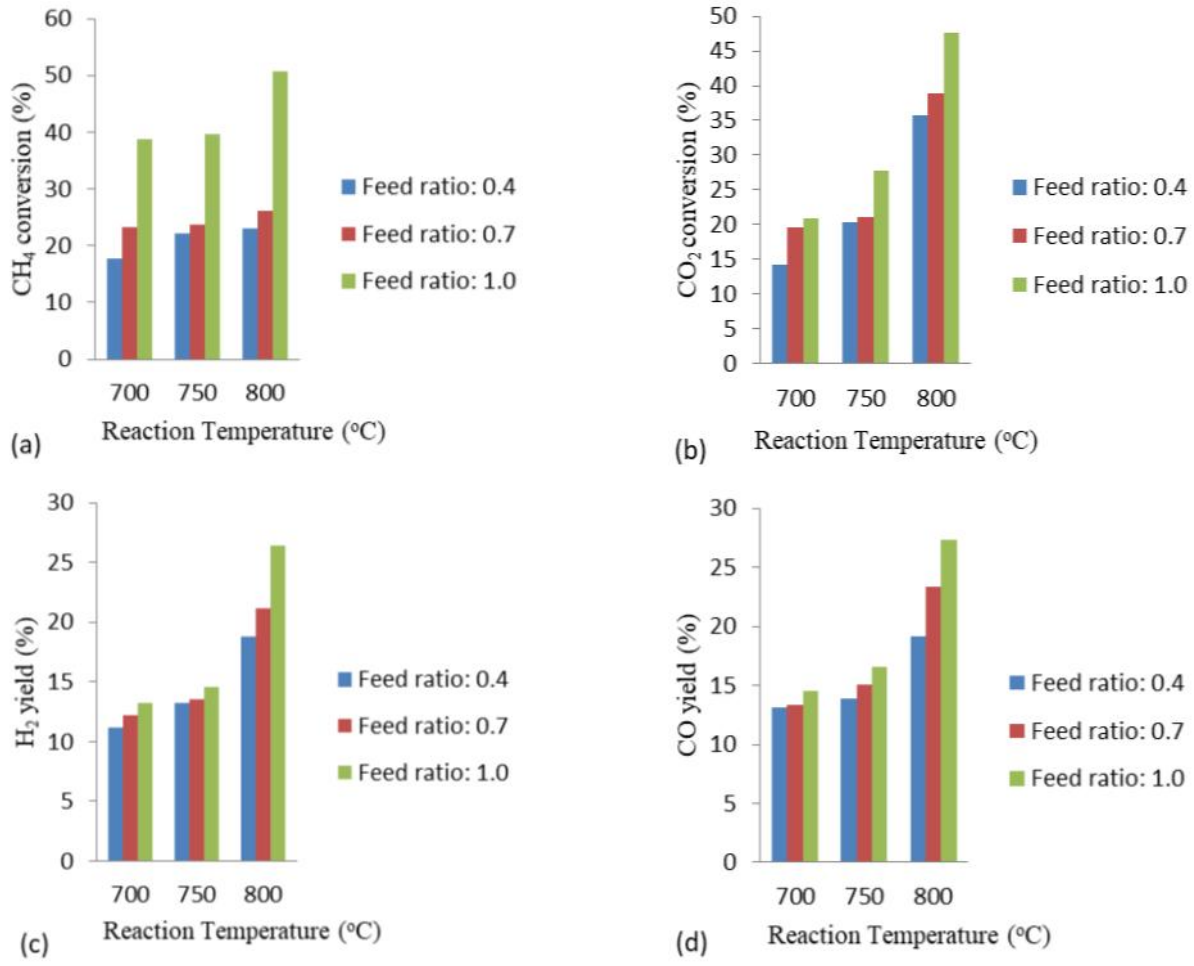

Figure 3. Catalytic performance of the 5% Ni/$CaFe_2O_4$ in methane dry reforming reaction (atmospheric pressure, GHSV of 30000 h^{-1})

and feed ratio (cf. Figure 3 (b)). Highest values of 50.7 % and 47.6 % were obtained for the CH_4 and CO_2 conversions at reaction temperature and feed ratio of 800 °C and 1.0, respectively. The higher value of CH_4 conversion obtained could be as result of side reaction such as methane cracking [19]. Furthermore, both the H_2 and CO yields increased with reaction temperature and feed ratio as shown in Figures 3 (c) and (d) resulting to the highest values of 26.42 % and 27.31 %, respectively.

Furthermore, the catalytic activity of the 10% $Ni/CaFe_2O_4$ catalyst is shown in Figure 4. The catalyst also displayed impressive activity in terms of CH_4 and CO_2 conversion as well as H_2 and CO yield. It is noteworthy that the CH_4 conversion increases with both feed ratio and temperature. Similarly, CO_2 conversion also increases with feed ratio and temperature. However, the increase in the CH_4 conversion was not pronounced at temperature of 700 and 800 °C using feed ratio of 0.4. The methane dry reforming over 10% $Ni/CaFe_2O_4$ demonstrated highest CH_4 and CO_2 conversions of 67.97 and 66.38%, respectively, which was higher compared to the performance of 5% $Ni/CaFe_2O_4$. The lower CO_2 conversion obtained over 10% $Ni/CaFe_2O_4$ might be due to the possibility of influence of side reaction such as methane cracking which leads to higher conversion of CH_4. The 10% $Ni/CaFe_2O_4$ catalyst also show an interesting performance in terms of the yield of the products (H_2 and CO). Both the H_2 and CO yield increases with feed ratio and temperature.

The methane dry reforming reaction over the 10% $Ni/CaFe_2O_4$ catalyst gave highest H_2 and CO yields of 35.34 % and 38.31 %, respectively at feed ratio of 1.0 and temperature of 800 °C. The higher values of CO yield obtained compare to that of H_2 indicate the possibility of the influence of reverse Boudouard reaction which increases the yield of the CO in addition to the product obtained from the dry reforming reaction.

The catalytic performance of 15% $Ni/CaFe_2O_4$ catalysts in methane dry reforming is depicted in Figure 5. The catalysts showed

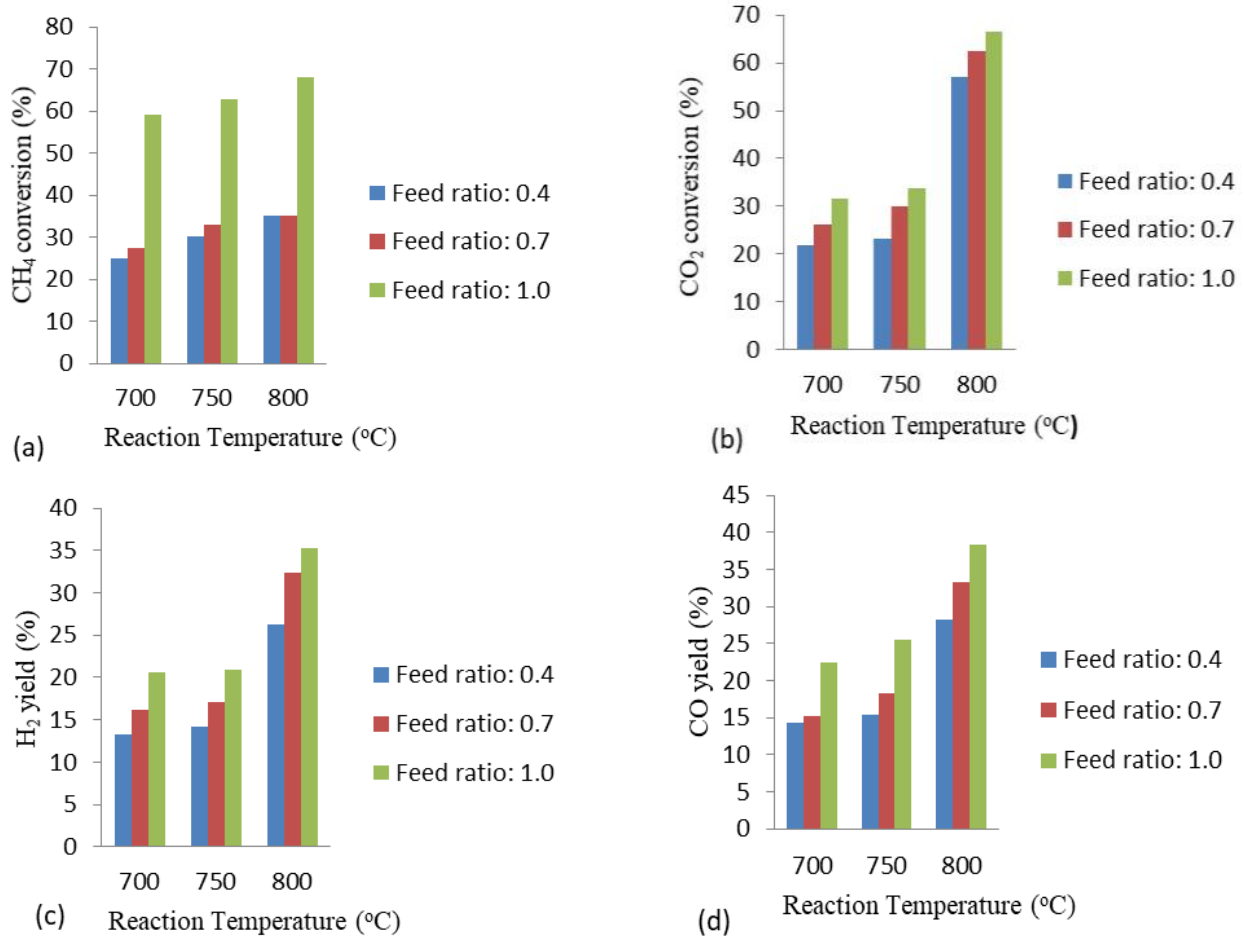

Figure 4. Catalytic performance of the 10% $Ni/CaFe_2O_4$ in methane dry reforming reaction (atmospheric pressure, GHSV of 30000 h^{-1})

an interesting activity in terms of CH_4 and CO_2 conversion as well as H_2 and CO yield. The CH_4 conversion using feed ratio of 0.4 showed slight increase in the temperature range of 700-800 ^oC. However, the increase in the CH_4 conversion with the temperature became pronounced at feed ratio ranged 0.7-1.0.

The catalytic activity resulted to highest CH_4 conversion of 90.04 % at feed ratio of 1.0 and temperature of 800 ^oC. Similarly, CO_2 conversion also increases with reaction temperature and feed ratio resulting to highest conversion of 87.60 % which is lower compared to that of CH_4. The lower conversion of CO_2 obtained implies that there might be possibility of influence of side reaction, such as methane cracking, which leads to higher conversion of CH_4 [20]. The highest values of CH_4 and CO_2 conversions obtained for the 15% $Ni/CaFe_2O_4$ catalyst is this study is comparable with conversion values of ~91 % and ~92 % obtained for CH_4 and CO_2 by Du *et al.* [21] using Ni/CeO_2 catalyst. The CH_4 and CO_2 conversions obtained in this study is higher than 78 % and 60 % reported by Sutthiumporn [22] using alkaline promoted Ni/La_2O_3 catalyst. The variation in the catalytic performance could be as a result of the difference in the catalysts physicochemical properties. The 15% $Ni/CaFe_2O_4$ catalyst also shows an interesting performance in terms of the yield of the products (H_2 and CO). Both the H_2 and CO yields increase with feed ratio and temperature.

The catalytic activity of the 15% $Ni/CaFe_2O_4$ catalyst gives highest H_2 and CO yields of 73.41 % and 74.43 % respectively at feed ratio of 1.0 and temperature of 800 ^oC. The higher values of CO yield obtained compare to that of H_2 indicated the possibility of the influence of reverse Boudouard reaction which increases the yield of the CO in addition to the product obtained from the dry reforming reaction [23].

3.3 Catalyst characterization

The thermal analysis profile of the uncalcined 15%wt $Ni/CaFe_2O_4$ catalyst is depicted in Figure 6. Typically, the temperature pro-

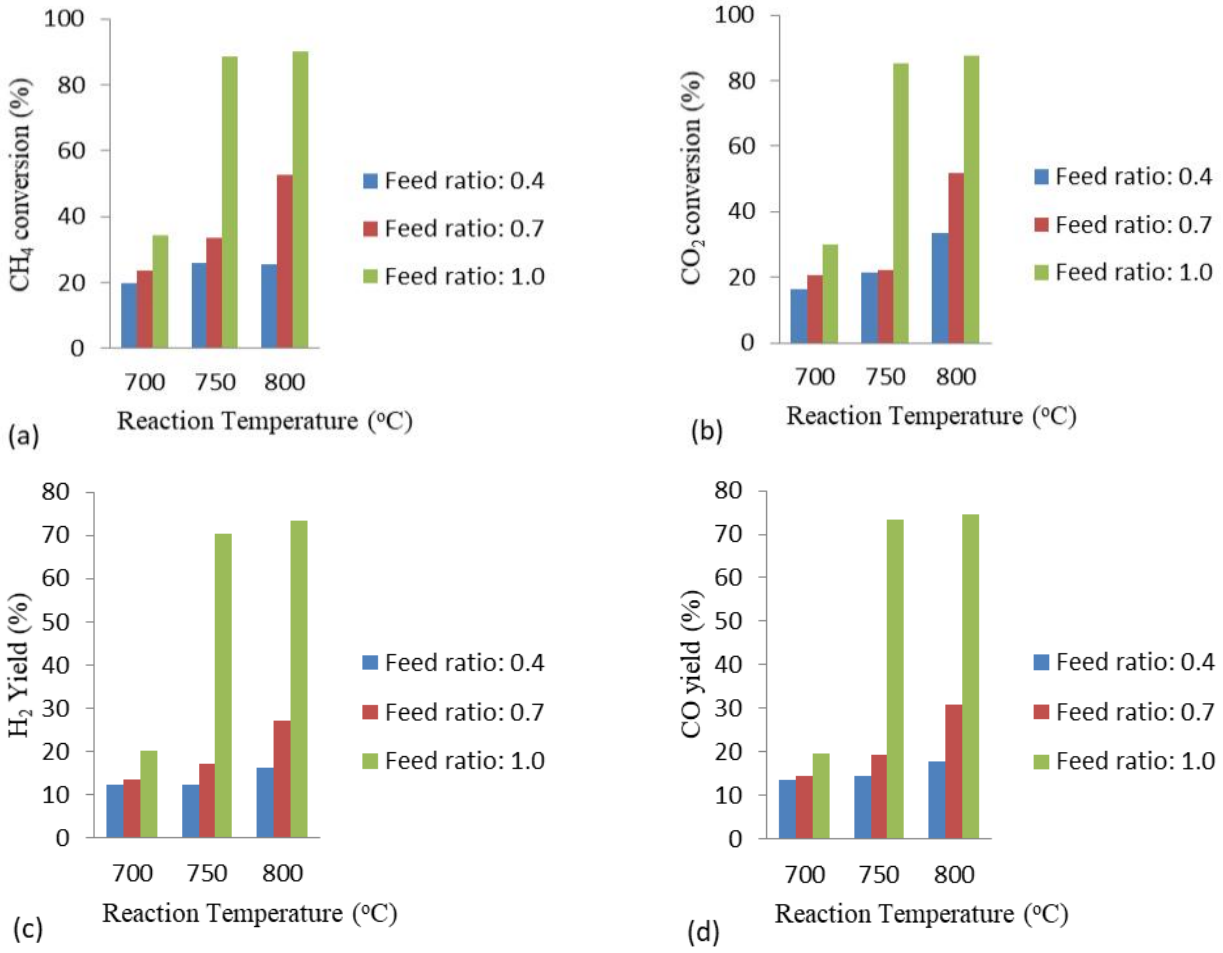

Figure 5. Catalytic performance of the 15% $Ni/CaFe_2O_4$ in methane dry reforming reaction (atmospheric pressure, GHSV of 30000 h^{-1})

grammed calcination showing the TG and the DTG can be group into four stages represented by peaks I-IV. Peak I and II at temperature range of 100-140 °C can be attributed to the loss of physical and hydrated water. Peaks III and VI center at temperature of 300 and 480 °C respectively can be attributed to the thermal decomposition of nitrate compounds present in the catalyst sample leading to the formation of NiO. Interestingly, the TG became flattened at temperature > 500 °C signifying the absence of any other components in the catalyst aside NiO and $CaFe_2O_4$ which is consistent with the XRD pattern shown in Figure 7 [24]. This justified the choice of the calcinating the dried freshly prepared 15%wt Ni/$CaFe_2O_4$ catalyst at temperature > 500 °C.

Figure 7 depicts the XRD analysis of the $CaFe_2O_4$ and the reduced 15%wt Ni/$CaFe_2O_4$ catalyst. Interestingly, the $CaFe_2O_4$ and Ni/15%wtNi/$CaFe_2O_4$ catalyst match well with the documented XRD data of $CaFe_2O_4$ (ICDD card No. 03-065-1333) and Ni (ICDD card No. 00-001-1258), an indication of the formation of well-crystallized catalyst. The orthorhombic structure of the $CaFe_2O_4$ can be identified at 2θ = 32.12° (111), 33.17° (004), 34.30° (302), 42.86° (311), 43.82° (213), 44.82° (304), 49.40° (214), 50.97° (006), 52.57° (404), 60.69° (116), 61.06° (600), 63.46° (216), 65.16° (513), 69.41° (610), 70.28° (108), 75.08° (613) and 78.18° (118) [17]. While that of cubic structure of Ni° can be identified at 2θ = 12.15° (110), 23.00° (220), 35.99° (101), 41.43° (100) 47.12° (130), 47.92° (131), 51.12° (103), 58.06° (201), 59.33° (104), 66.35° (014) and 78.15° (105). Scherrer's expression was employed to estimate the particle size diameter of the sharpest peak of the $CaFe_2O_4$ and Ni° (2θ = 42.86° and 78.18°, respectively) given as 22.47 and 27.26 nm, respectively.

The morphology and the elemental composition of the 15wt%Ni/85wt%$CaFe_2O_4$ represented by the FESEM image and EDX micrograph are shown in Figure 8. It is noteworthy that the SEM image of the catalyst displayed weak agglomerated small spherical-shaped particles. The observed particle diameter of the catalyst was estimated at four different spots and recorded as 73.65, 43.41, 56.36, and 68.02 nm. Moreover, the elemental make-up of the 15wt% Ni/85wt%$CaFe_2O_4$ catalyst (Ni, Ca, Fe and O) obtained from the EDX micrograph (Figure 8 (b)) showed that Ni phase were well distributed on the $CaFe_2O_4$ support. Interestingly, there is a close agreement between the stipulated composition of the as-prepared catalyst and the values obtained from the EDX (Ni=15.45%, Ca+Fe+O= 84.65%).

The XPS spectra and the plot of the atomic concentration showing the oxidation state and the elemental composition of the catalyst are depicted in Figure 9 (a) and (b), respectively. It can be seen that all the elemental components such as Ni, Ca, Fe, and O of the 15wt%Ni/85wt%$CaFe_2O_4$ catalyst and their oxidation states are fully captured by the XPS. The presence of the elemental components corroborates the EDX and XRD analysis. The atomic concentrations of Ni, Ca, Fe, and O in the catalysts was estimated as 13.4 %, 7.5 %, 20.9 % and 57.8 %, respectively.

The N_2 phisorption analysis for the determination of the BET specific surface area and the BJH pore distribution is depicted in Figure 10. The obtained isotherm is typical of a Type-V with H3 hysteresis according to the IUPAC

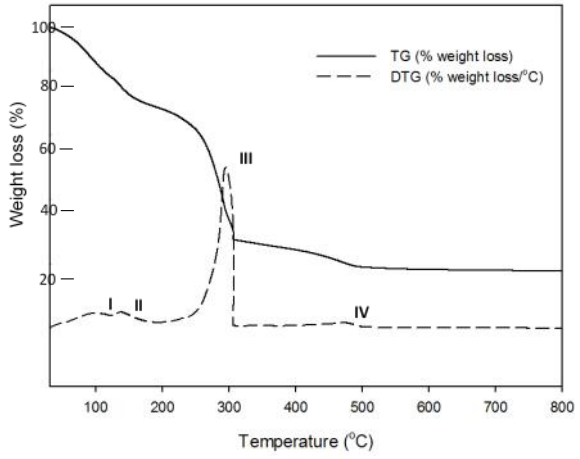

Figure 6. Temperature programmed calcination of the uncalcined fresh 15%wt Ni/$CaFe_2O_4$ catalyst

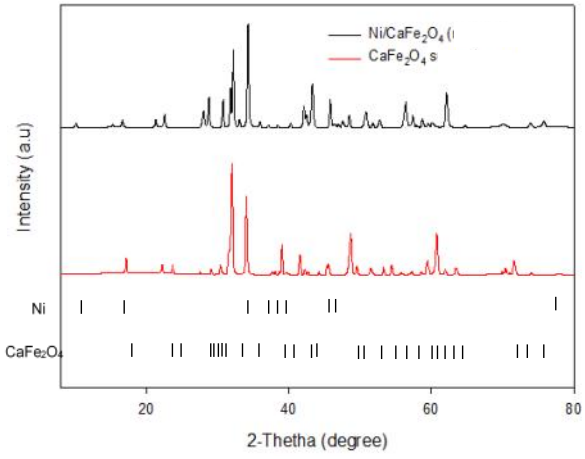

Figure 7. XRD pattern of $CaFe_2O_4$ and reduced 15%wtNi/$CaFe_2O_4$ catalyst

classification which is an indication of the formation of mesopores distributions within the catalyst sample. The specific surface area and the pore volume of the catalyst estimated using BET and BJH method are given a 5.13 m^2/g and 0.01 cm^3/g, respectively, which is typical of $CaFe_2O_4$-containing species [25].

The TPD profile of the 15 wt% Ni/85wt%$CaFe_2O_4$ catalyst using NH_3 and CO_2 as probe gases are depicted in Figure 11 (a) and (b), respectively. It can be seen that distinct desorption peaks at 665 °C and 660 °C was identified for the TPD-NH_3 and TPD-CO_2 profile, respectively. As a general rule, the desorption of a probe gas at lower temperature range (< 500 °C) signifies weak acid or basic site while desorption at a higher temperature range (> 500 °C) implies strong acid or basic site [26]. This implies that the 15wt%Ni/85wt%$CaFe_2O_4$ catalyst possesses both strong acid and basic sights which is advantageous for the activation of CH_4 and CO_2 during methane dry reforming [27].

The spectrum obtained from the analysis of the pure $CaFe_2O_4$ support and 15 wt% Ni/85wt%$CaFe_2O_4$ catalyst for the nature of chemical bond using FTIR are depicted in Figure 12. Interestingly, the FTIR spectrum revealed a characteristic structure of the $CaFe_2O_4$ support. The stretching vibration of OH^- signifying adsorbed water molecules can be identified at wavenumber ranged 3500-3000 cm^{-1}. Similarly, the stretching vibration C–O bond which represents adsorbed atmospheric CO_2 can be identified at 1544 -1284 cm^{-1}. Significantly, metallic bonds were observed at 805 and 692 cm^{-1} which can be attributed to the stretching vibration of Ca–O and Fe–O metal oxides bond in the $CaFe_2O_3$ support [28]. Moreover, the catalyst also exhibit stretching

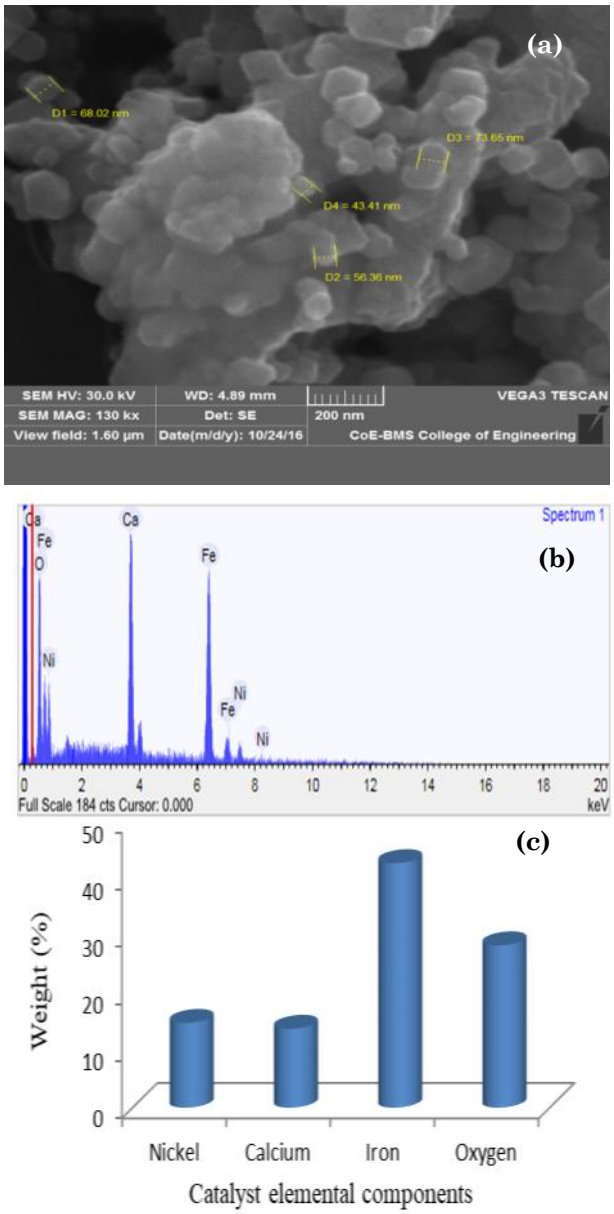

Figure 8. (a) FESEM image, (b) EDX micrograph, (c) elemental composition of the catalyst from EDX of the 15%wt Ni/$CaFe_2O_4$ catalyst

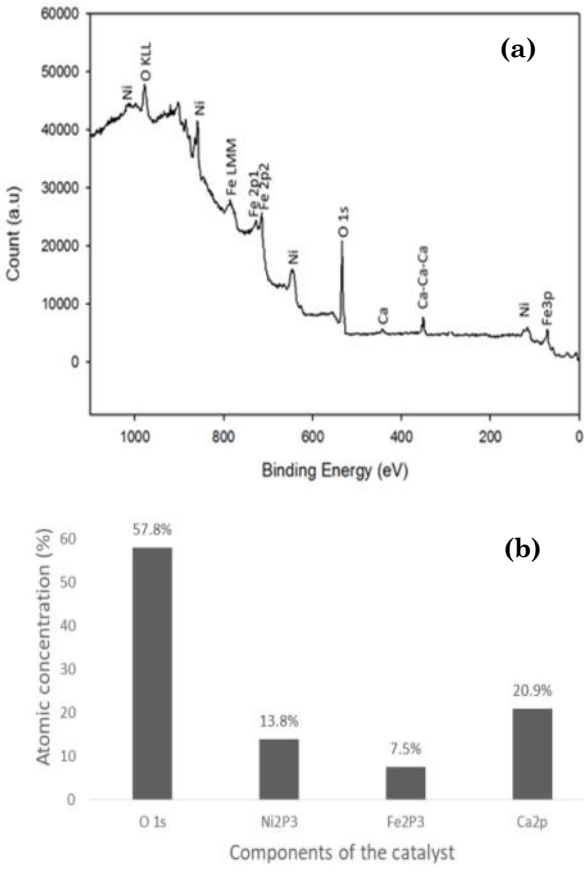

Figure 9. (a) The XPS profile of the 15%wt Ni/$CaFe_2O_4$ catalyst and (b) Elemental composition of the 15%wt Ni/$CaFe_2O_4$ catalyst

vibration Ca–O, Fe–O, and Ni–O bonds at bands at 803, 692, and 627 cm^{-1}, respectively. correspond to the Ca–O and Fe–O metal oxide bonds in the catalyst [29].

3.4 Interaction effect of feed ratio, metal loading and reaction temperature on the CH_4 conversion

In the full factorial design of experiments, three factors namely feed ratio, reaction temperature and metal loading were considered. The response and the contour plots showing the effects of feed ratio, reaction temperature and metal loading on the CH_4 are depicted in Figure 13. The response plots show the effect of the factors on the catalytic activities in terms of CH_4 conversion while the contour plots show the interaction between the factors as they influence the CH_4 conversion. Interestingly, the feed ratio, reaction temperature and metal loading show various degrees of influence on the CH_4 conversion (cf. Figure 13 (a)). However, the CH_4 conversion is mostly influenced by the reaction temperature which is consistent with Arrhenius observation [30]. This observation is consistent with the findings of Serrano-Lotina and Daza [31] who reported the influence of reaction temperature ranged 450-850 °C on CH_4 conversion. Furthermore, the three factors displayed different level of interactions as shown in Figures 13 (a)-(c). It can be seen that the interaction between the feed ratio and the reaction temperature has more impact on the CH_4 conversion at feed ratio ranged 0.7-1.0 and reaction temperature of 800 °C. Similarly, the interaction between the feed ratio and the metal loading show significant influence on the CH_4 conversion at metal loading of 10 % and feed ratio ranged 0.7-1.0. The effect of the interaction between the metal loading and the reaction temperature was significant at reaction temperature and metal loading of 800 °C and 10 %, respectively.

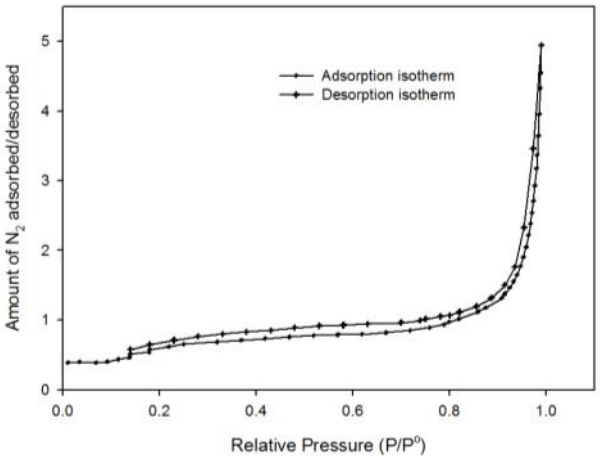

Figure 10. N_2 adsorption-desorption isotherm of the 15%wtNi/$CaFe_2O_4$ catalyst

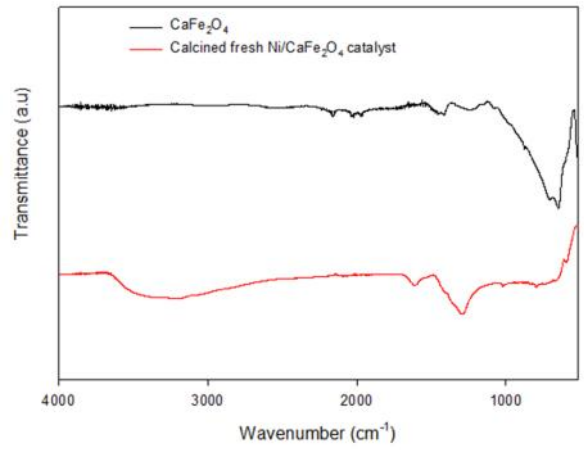

Figure 12. FTIR spectrum of the fresh 15%wt Ni/$CaFe_2O_4$ catalyst before and after calcination

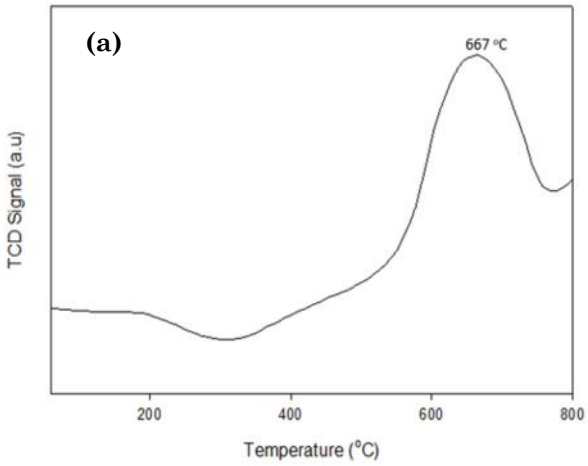

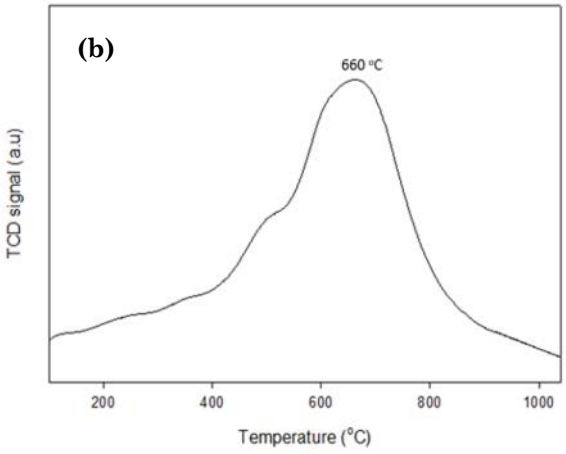

Figure 11. TPD profiles of the 15wt% Ni/$CaFe_2O_4$ catalyst using (a) NH_3 and (b) CO_2 as probing gases

3.5 Interaction effect of feed ratio, metal loading and reaction temperature on the CO_2 conversion

The interaction effects of the reactant feed ratio, metal loading and the dry reforming reaction temperature on CO_2 conversion are depicted in Figure 14. The three factors displayed varying level of interaction effect on the CO_2 conversion. It can be seen that both the feed ratio and the reaction temperature have significant effects on the CO_2 conversion (Figure 14 (a)). The CO_2 conversion increases with feed ratio and reaction temperature. The interaction between the feed ratio and the reaction temperature shows a greater effect on the CO_2 conversion at unity feed ratio and reaction temperature of 800 ^oC as indicated by the red portion of the plot. This trend is in agreement with the findings of Serrano-Lotina and Daza [31] who obtained the highest value of CO_2 conversion at reaction temperature and feed ratio

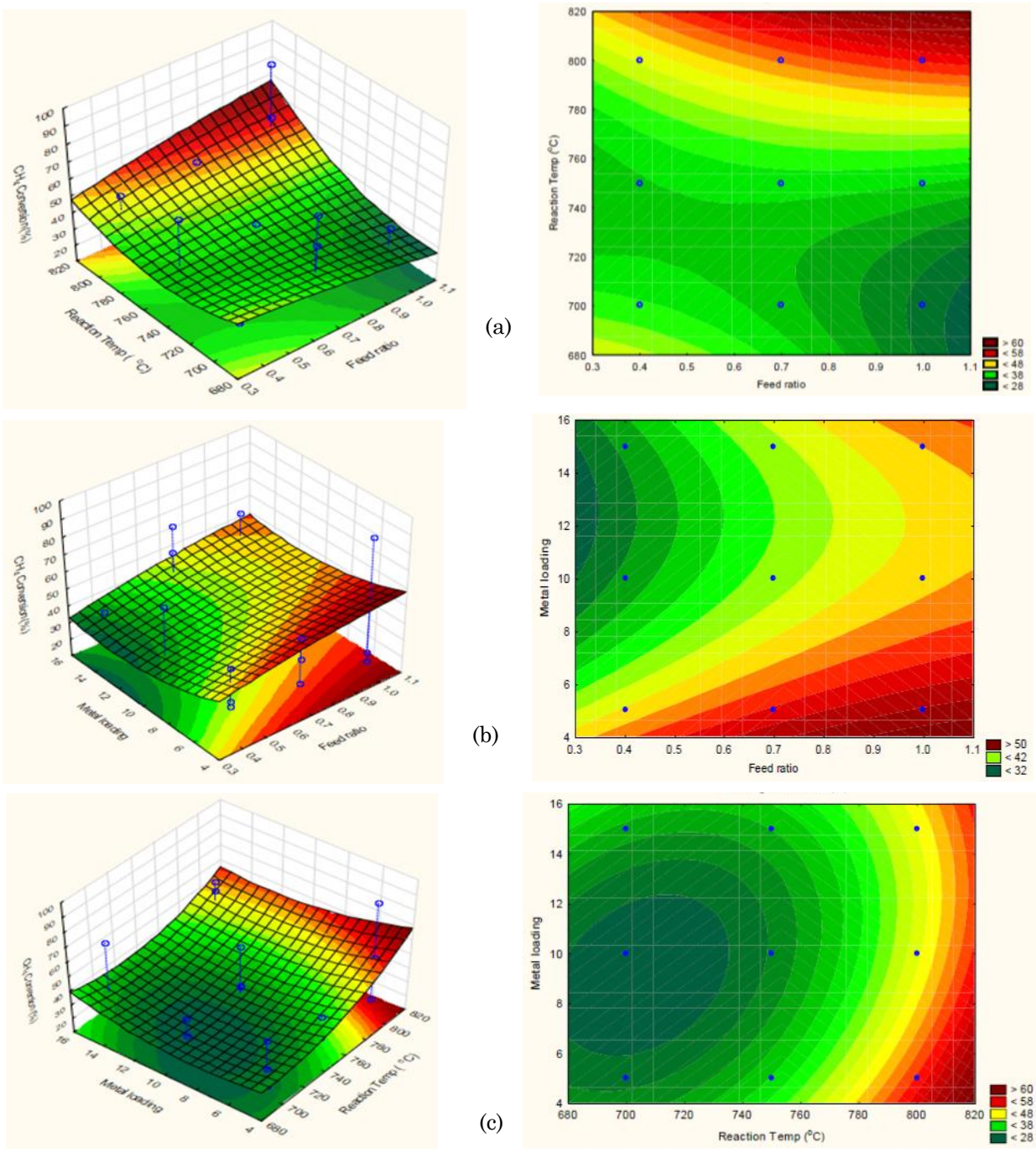

Figure 13. Response and contour plots for CH_4 conversion (a) Effects of feed ratio and reaction temperature (b) Effect of metal loading and feed ratio (c) Effect of metal loading and reaction temperature at atmospheric condition and GHSV of 30000 h^{-1}

of 800 °C and 1, respectively, in methane dry reforming over Ni/Al_2O_3 catalyst. Contrary to the interaction between the reaction temperature and feed ratio, the interaction between the feed ratio and metal loading did not show pronounce effect on the CO_2 conversion. However, based on the interaction plot (Figure 14 (b)) the CO_2 conversion was only slightly influenced by the interaction between the feed ratio and metal loading at 1.0 and 10 %, respectively. Moreover, both metal loading and the reaction temperature have increasing effect on the CO_2 conversion (Figure 14(c)). It can also been seen that the interaction between the metal loading and the reaction temperature became stronger on the CO_2 conversion at metal loading and reaction temperature of 10 % and 800 °C, respectively as indicated by the red portion of the plot.

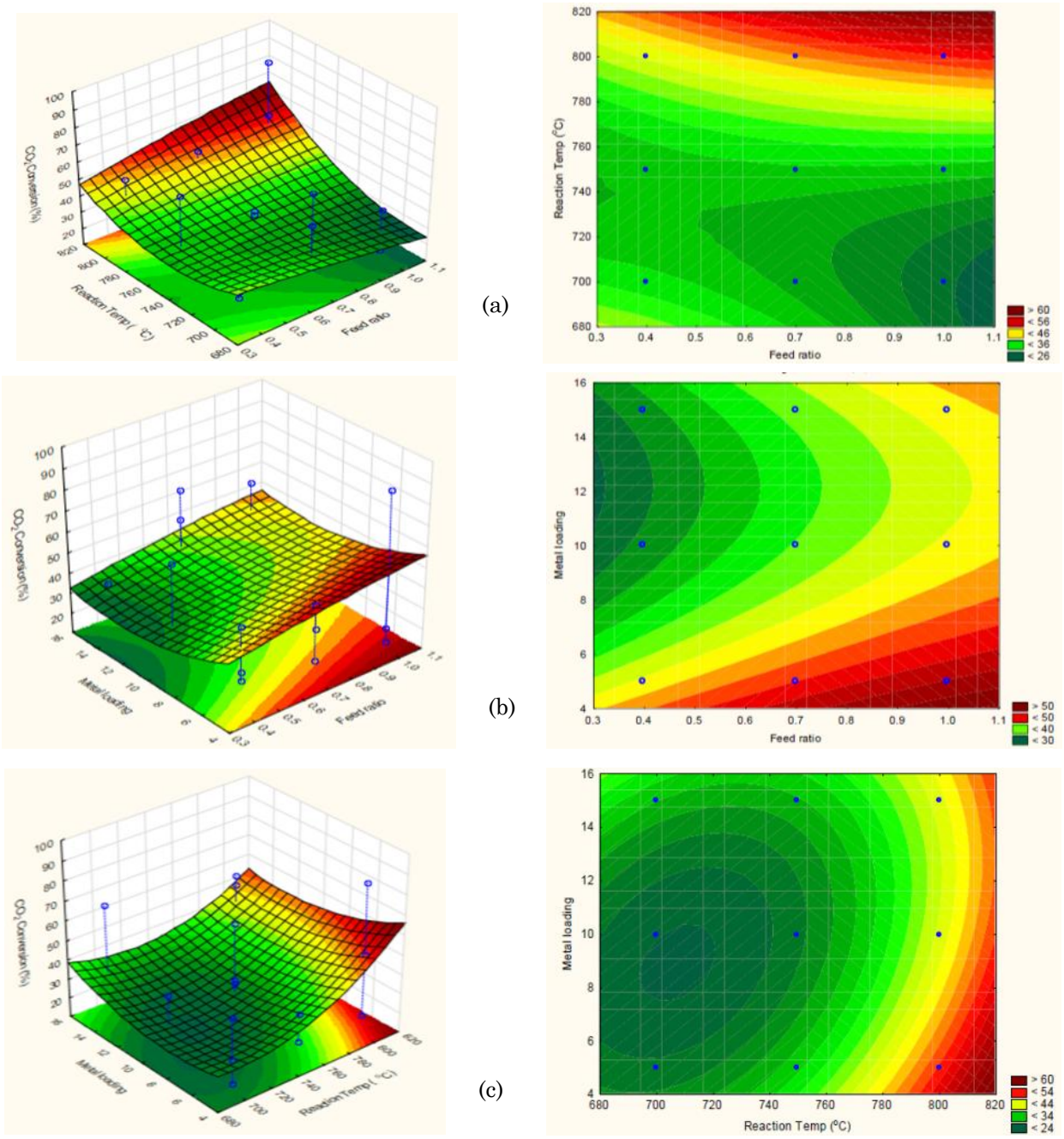

Figure 14. Response and contour plots for CO_2 conversion (a) Effects of feed ratio and reaction temperature (b) Effect of metal loading and feed ratio (c) Effect of metal loading and reaction temperature at atmospheric condition and GHSV of 30000 h^{-1}

3.6 Interaction effect of feed ratio, metal loading and reaction temperature on the H_2 yield

Figure 15 show the interaction effects of feed ratio, metal loading and the reaction temperature on the H_2 yield. The three factors vary in level of interaction effects on the H_2 yield. There is a significant interaction effect between the feed ratio and the reaction temperature as evident from the increasing trend of the H_2 yield (Figure 15 (a)). However, this interaction has greater effect on the H_2 yield at unity feed ratio and reaction temperature of 800 ^oC. The metal loading and feed ratio did not however show good interaction compared to the interaction between feed ratio and reaction temperature. This interaction between the feed ratio and the metal loading shows significant effect on the hydrogen yield at all range of the feed ratio and 10 % metal loading. The interaction

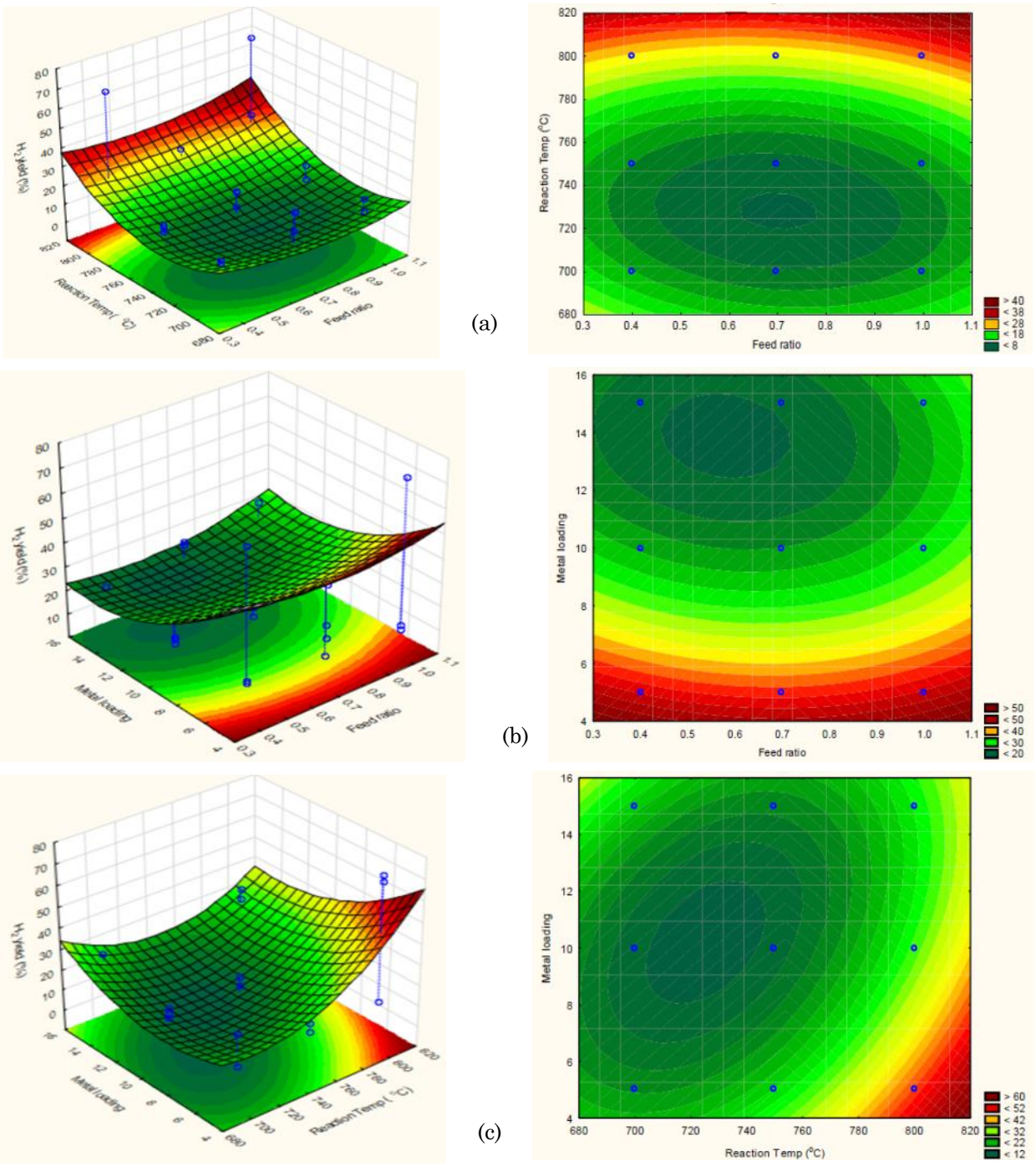

Figure 15. Response and contour plots for H_2 yield (a) Effects of feed ratio and reaction temperature (b) Effect of metal loading and feed ratio (c) Effect of metal loading and reaction temperature at atmospheric condition and GHSV of 30000 h^{-1}

between the reaction temperature and metal loading also shows greater effect on the H_2 yield at metal loading of 10 % and reaction temperature of 800 ^oC.

3.7 Interaction effect of feed ratio, metal loading and reaction temperature on the CO yield

The interaction effects of the reactant feed ratio, metal loading and reaction temperature on the CO yield are depicted in Figure 16. The three factors have various degrees of interaction effects on the CO yield. The temperature and the feed ratio appear to have higher interaction effect on the CO yield as indicated by red portion of Figures 16 (a). The CO yield increases with the dry reforming reaction temperature while both the feed ratio and the metal loading show less interaction effect on the CO yield. The interaction effect of the reac-

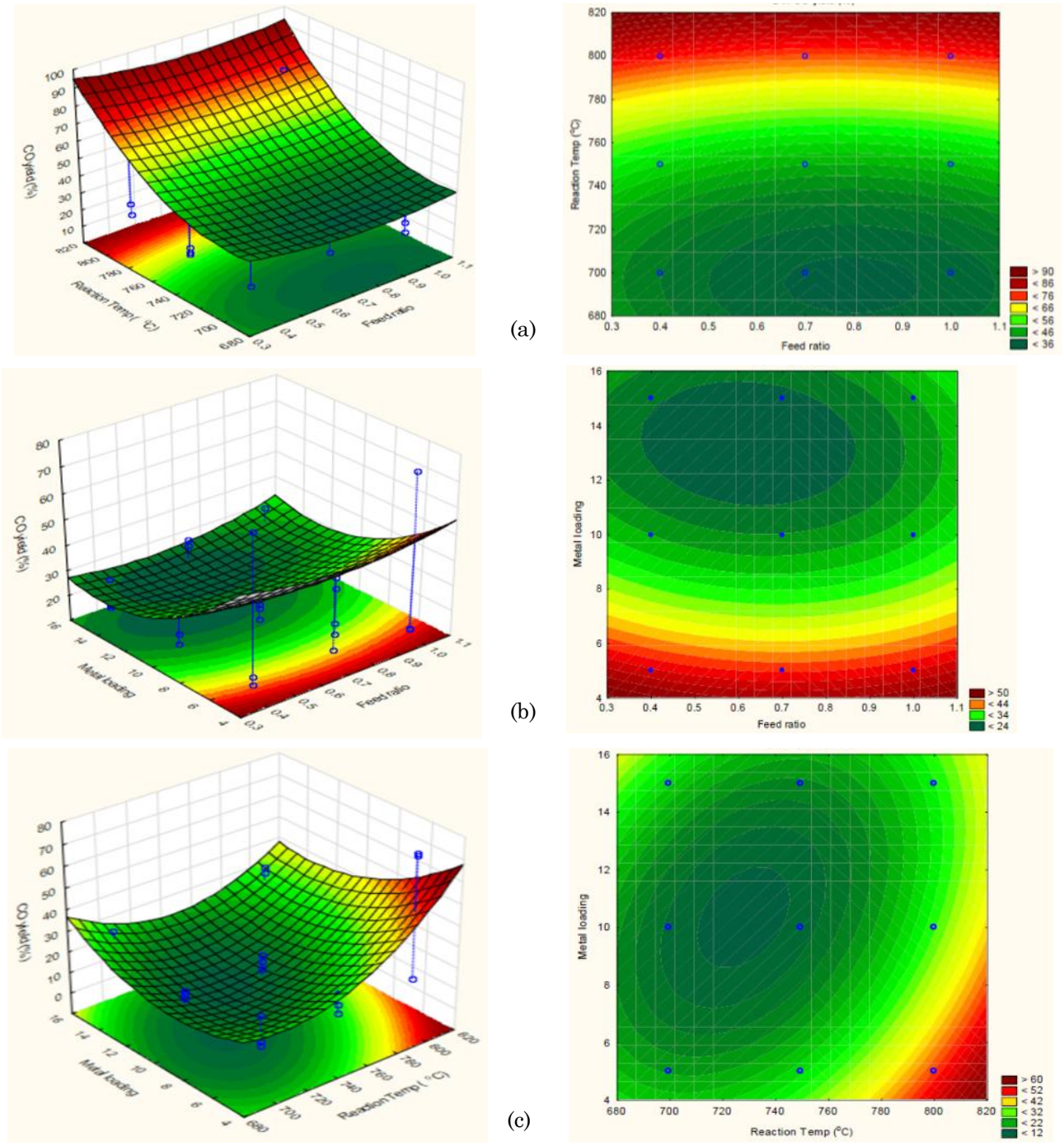

Figure 16. Response and contour plots for CO yield (a) Effects of feed ratio and reaction temperature (b) Effect of metal loading and feed ratio (c) Effect of metal loading and reaction temperature at atmospheric condition and GHSV of 30000 h^{-1}

tion temperature on the CO yield was greatest at 800 ^{o}C as indicated on the red portion of Figure 16 (b). It can be seen from the red portion of Figures 16 (a)-(c) that the feed ratio shows stronger interaction effect at higher temperature and 10% metal loading.

4. Conclusions

Dry reforming of methane over novel Co- and Ni/$CaFe_2O_4$ catalysts was carried out for the production of syngas. The catalysts were synthesized using wet-impregnation method and subsequently pre-screened by testing the catalytic performance in methane dry reforming reaction. The pre-screening test showed that the Ni/$CaFe_2O_4$ has the best catalytic performance in terms of conversion and yields. Hence, Ni was selected as the active metal to be dispersed on the $CaFe_2O_4$ support. Subsequently, full factorial design of experiment was employed to further develop the $CaFe_2O_4$ supported Ni catalyst. The interaction effects of factors such as metal loading (5-15%), feed ratios (0.4-1.) and reaction temperature (700-800 ^{o}C) were considered on the performance of the Ni/$CaFe_2O_4$ in terms of CH_4 and CO_2 conversion as well as H_2 and CO yield. The Ni/$CaFe_2O_4$ catalyst showed a promising performance using metal loading of 15 %, reaction temperature of 800 ^{o}C and unity feed ratio with highest CH_4 and CO_2 conversions of 90.04 and 87.67 %, respectively. The 15wt% Ni/$CaFe_2O_4$ catalyst was subsequently characterized for its physicochemical properties by TGA, XRD, FE-SEM, EDX, XPS, N_2-physisorption, and FTIR. The methane dry reforming over the 15wt% Ni/$CaFe_2O_4$ gave syngas ratio of 0.99 making it suitable as a chemical intermediate for the production of oxygenated fuel via Fischer-Tropsch synthesis.

Acknowledgements

M. Anwar Hossain gratefully acknowledge the Doctoral Scholarship (DSS) and the PGRS grant offered by Universiti Malaysia Pahang.

References

[1] Anderson, T.R., Hawkins, E., Jones, P.D., (2016). CO_2, the Greenhouse Effect and Global Warming : from the Pioneering Work of Arrhenius and Callendar to Today's Earth System Models. *Endeavour*. 40(3): 178-187. doi:10.1016/j.endeavour.2016.07.002.

[2] Basha, M.N., Malik, A., Peedikakkal, P. (2016). Carbon Capture by Physical Adsorption : Materials, Experimental Investigations and Numerical Modeling and Simulation-A Review. *Appl Energy*, 161: 225-255.

[3] Ayodele, B.V., Khan, M.R., Cheng, C.K. (2016). Greenhouse Gases Mitigation by CO_2 Reforming of Methane to Hydrogen-Rich Syngas Using Praseodymium Oxide Supported Cobalt Catalyst. *Clean Technol. Environ, Policy*, 19: 1-13.

[4] Ayodele, B.V., Khan, M.R., Cheng, C.K. (2017). Greenhouse Gases Abatement by Catalytic Dry Reforming of Methane to Syngas over Samarium Oxide-Supported Cobalt Catalyst. *Int J Environ Sci Technol*, 1-14. 14(12): 2769-2782

[5] Ayodele, B.V., Khan, M.R., Cheng, C.K. (2016). Production of CO-rich Hydrogen Gas from Methane Dry Reforming over Co/CeO_2 Catalyst. *Bull. Chem. React. Eng. Catal.*, 11: 210-219.

[6] Sidik, S.M., Triwahyono, S., Jalil, A.A., Majid, Z.A., Salamun, N., Talib, N.B. (2016). CO_2 Reforming of CH_4 over Ni-Co/MSN for Syngas Production: Role of Co as a Binder and Optimization Using RSM. *Chem. Eng. J.*, 295: 1-10.

[7] Abatzoglou, N., Fauteux-lefebvre, C. (2016). Review of Catalytic Syngas Production Through Steam or Dry Reforming and Partial Oxidation of Studied Liquid Compounds. *WIREs Energy Env.* 5(2): 169-187

[8] Lee, J.H., You, Y-W., Ahn, H.C., Hong, J.S., Kim, S.B., Chang, T.S. (2014). The Deactivation Study of Co–Ru–Zr Catalyst Depending on Supports in the Dry Reforming of Carbon Dioxide. *J. Ind. Eng. Chem.*, 20: 284-289.

[9] Ayodele, B.V., Cheng, C.K. (2015). Process Modelling, Thermodynamic Analysis and Optimization of Dry Reforming, Partial Oxidation and Auto-Thermal Methane Reforming for Hydrogen and Syngas Production. *Chem. Prod. Process Model.*, 10: 211-220.

[10] Pakhare, D., Spivey, J. (2014). A Review of Dry (CO_2) Reforming of Methane over Noble Metal Catalysts. *Chem. Soc. Rev.*, 43(22): 7813-7837

[11] Budiman, A.W., Song, S.H., Chang, T.S., Choi, M.J. (2016). Preparation of a High Performance Cobalt Catalyst for CO_2 Reforming of Methane. *Adv. Powder Technol.* 27(2): 584-590

[12] Luu, Q., Ha, M., Armbruster, U., Atia, H., Schneider, M., Lund, H. (2017). Development of Active and Stable Low Nickel Content Catalysts for Dry Reforming of Methane. *Catalysts*, 7: 1-17.

[13] Budiman, A.W., Song, S-H., Chang, T-S., Shin, C-H., Choi, M-J. (2012). Dry Reforming of Methane Over Cobalt Catalysts: A Litera-

ture Review of Catalyst Development. *Catal. Surv. Asia*, 16: 183-197.

[14] Itkulova, S.S., Zakumbaeva, G.D., Nurmakanov, Y.Y., Mukazhanova, A.A., Yermaganbetova, A.K. (2014). Syngas Production by Bi-reforming of Methane over Co-based Alumina-Supported Catalysts. *Catal. Today*, 228: 194-198.

[15] Ayodele, B.V., Khan, M.R., Cheng, C.K. (2015). Syngas Production from CO_2 Reforming of Methane over Ceria Supported Cobalt Catalyst: Effects of Reactants Partial Pressure. *J. Nat. Gas Sci. Eng.* 27: 1016-1023

[16] Talkhoncheh, S.K., Haghighi, M. (2015). Syngas Production via Dry Reforming of Methane over Ni-Based Nanocatalyst over Various Supports of Clinoptilolite, Ceria and Alumina. *J. Nat. Gas Sci. Eng.*, 23: 16-25.

[17] Zhang, Z., Wang, W. (2014). Solution Combustion Synthesis of $CaFe_2O_4$ Nanocrystal as A Magnetically Separable Photocatalyst. *Mater. Lett.*, 133: 212-215.

[18] Xue, B., Luo, J., Zhang, F., Fang, Z. (2014). Biodiesel Production from Soybean and Jatropha Oils by Magnetic $CaFe_2O_4$-$Ca_2Fe_2O_5$-based Catalyst. *Energy*, 68: 584-591.

[19] Laosiripojana, N., Sutthisripok, W., Assabumrungrat, S. (2005). Synthesis Gas Production From Dry Reforming of Methane over CeO_2 Doped Ni/Al_2O_3: Influence of the Doping Ceria on the Resistance toward Carbon Formation. *Chem. Eng. J.*, 112: 13-22.

[20] Verykios, X.E. (2003). Catalytic Dry Reforming of Natural Gas for the Production of Chemicals and Hydrogen. *Int. J. Hydrogen Energy*, 28: 1045-1063.

[21] Du, X., Zhang, D., Shi, L., Gao, R., Zhang, J. (2011). Morphology Dependence of Catalytic Properties of Ni/CeO_2 Nanostructures for Carbon Dioxide Reforming of Methane. *J. Phys. Chem. C*, 116: 10009-10016.

[22] Sutthiumporn, K., Kawi, S. (2011). Promotional Effect of Alkaline Earth over Ni–La_2O_3 Catalyst for CO_2 Reforming of CH_4: Role of Surface Oxygen Species on H_2 Production and Carbon Suppression. *Int. J. Hydrogen Energy*, 36: 14435-14446.

[23] Haag, S., Burgard, M., Ernst, B. (2007). Beneficial Effects of the Use of A Nickel Membrane Reactor for the Dry Reforming of Methane: Comparison with Thermodynamic Predictions. *J. Catal.*, 252: 190-204.

[24] Brockner, W., Ehrhardt, C., Gjikaj, M. (2007). Thermal Decomposition of Nickel Nitrate Hexahydrate, $Ni(NO_3)_2 \cdot 6H_2O$, in Comparison to $Co(NO_3)_2 \cdot 6H_2O$ and $Ca(NO_3)_2 \cdot 4H_2O$. *Thermochim Acta*, 456: 64-68.

[25] Ikenaga, N.O., Ohgaito, Y., Suzuki, T. (2005). H_2S Absorption Behavior of Calcium Ferrite Prepared in the Presence of Coal. *Energy and Fuels*, 19: 170-179.

[26] Pino, L., Vita, A., Cipitì, F., Laganà, M., Recupero, V. (2011). Hydrogen Production by Methane Tri-reforming Process over Ni–ceria Catalysts: Effect of La-doping. *Appl. Catal. B Environ.*, 104: 64-73.

[27] Pakhare, D., Spivey, J. (2014). A Review of Dry (CO_2) Reforming of Methane over Noble Metal Catalysts. *Chem. Soc. Rev.* 43(22): 7813-7837

[28] Khanna, L., Verma, N.K. (2013). Synthesis, Characterization and in Vitro Cytotoxicity Study of Calcium Ferrite Nanoparticles. *Mater. Sci. Semicond. Process.*, 16: 1842-1848.

[29] Šarić, A., Musić, S., Nomura, K., Popović, S. (1999). FT-IR and 57Fe Mössbauer Spectroscopic Investigation of Oxide Phases Precipitated from $Fe(NO_3)_3$ Solutions. *J. Mol. Struct.*, 480-481: 633-636.

[30] Clark, T.C., Dove, J.E. (1973). Examination of Possible Non-Arrhenius Behavior in the reactions. *Can. J. Chem.*, 51:2147-2154.

[31] Serrano-Lotina, A., Daza, L. (2014). Influence of the Operating Parameters over Dry Reforming of Methane to Syngas. *Int. J. Hydrogen Energy*, 39: 4089-4094.